APPLICATION OF AN ACTIVE CONTOUR MODEL FOR EXTRACTION OF FUZZY AND BROKEN IMAGE EDGES

PIOTR SZCZYPIŃSKI and PAWEŁ STRUMIŁŁO
Institute of Electronics, Technical University of Łódź,
Stefanowskiego 18/22, 90-537 Łódź

Abstract. The method of an active contour model (popularly termed *snake*) for extraction of image edges is presented in the paper. The main strength of the method is that it yields continuous contours even if the image edge/boundary information is fuzzy or fragmented. Two modifications to the original active contour model are proposed and explained in the paper. First of the modifications simplifies the original method [6] and makes it faster in computer implementation while retaining its performance. Second modification introduces novel method of contour construction which improves active contour capabilities in detecting complex curve shapes, e.g. spirals. Results are presented which demonstrate performance of the discussed edge detection methods on a number of artificial test images and on images derived from echoardiographic scans and X-ray scans of grains.

Keywords: machine vision, edge detection, active contour model.

1. Introduction

One of the initial and fundamental stages of an image analysis procedure is detection of characteristic image regions which could serve as a basis for decomposing (segmenting) visual information into objects of interest and their background. Image edges are usually used as these characteristic regions which are defined as loci of abrupt changes in image brightness. They can be extracted by means of various types of spatial image transformation techniques. The most commonly used edge finding techniques are the gradient-based Prewitt, Sobel, and Laplace detectors [1]. Also, other edge finding methods like second derivative zero-crossing detector [2] or a computational approach based on the Canny criteria [3] were reported. However, due to common image features like texture, noise, image blur or other anomalies, like non-uniform scene illumination, edge finding techniques frequently fail in producing confident results. Continuous image boundaries present in the source image may be represented by broken edge fragments or may not be detected at all. Also, in some cases, further utilisation of edge information can be

hindered by the fact that detected edges can be a few pixels wide. Finally, the detected edges may be false edges.

There has been a number of edge linking methods proposed to account for poorly represented image boundaries [8, 14]. These approaches, however, add an extra processing stage to the edge detection task. Also, another method based on Hough transform, has been employed for contour finding [5]. In spite of its robustness, this approach has not gained wider acceptance due to its high computational cost and high computer storage requirements.

This paper reports an alternative, global approach to the problem of contour extraction. It is based on the so called *active contour model* (also termed *snake*), first proposed in [6]. This clever edge finding scheme is particularly well suited for extraction of fuzzy and weak image edges. It has proved to be capable of interpolating the contour line between distant edge points and produce smooth continuation of broken contour fragments. Also, edges generated using this method are one pixel wide, which makes this form of edge representation precise and straightforward for further analysis.

The method of an active contour model, has become an established and important technique for locating image boundaries in computer vision applications. Recently, a number of papers related to this subject have appeared in which authors report some improvements [10, 13] and extensions of the original method [5]. Also this paper, which summarises the results obtained in [16], in more detail than communicated earlier in [15], reports novel modifications of the originally developed active contour model. First, the concept of the active contour model is introduced and its algorithmic implementation to the problem of image contour extraction is described. Then, two modifications of the active contour model are introduced and discussed. Achieved improvements of the method are demonstrated on a number of artificial test images and real world images such as echocardiographic images and X-ray images of grains.

2. An active contour model and its discrete implementation

An active contour may be viewed as a mathematical model of a deformable curve made up of flexible material [6]. In an image analysis context, an active contour is a flat curve, which can dynamically change its shape in order to match it to the geometry of salient image regions like edges or boundaries. The concept of contour shape formation for matching image edges is explained in Fig. 1. The objective of contour movements is to find the best fit, in terms of some cost function, as a trade-off between the contour curvature and the boundary of the image object under analysis. In [6] the potential energy function of the active contour has been proposed to play the role of this cost function. This energy function is given by the following integral equation:

$$E_{snake} = \int_0^{S_m} \left[E_{int}(v(s)) + E_{ext}(v(s)) + E_{image}(v(s)) \right] ds \qquad (1)$$

where the position of a snake is described parametrically by $v(s)=(x(s), y(s))$, E_{int} represents internal potential energy of the contour, E_{ext} is the energy which models external constraints

imposed onto the contour shape, and E_{image} represents the energy derived from image features, e.g. image brightness distribution.

Contour energy potential function (1) is constructed in such a way that its minimum value corresponds to the contour shape which matches the curvature of the sought image edges or boundaries. Hence, the task of extracting image boundaries by means of an active contour model can be defined as the optimisation problem, in which the minimum of the contour energy is searched for. However, in practical computer vision applications direct minimisation of equation (1) is seldom used. This would require iterative computations of the optimised function (or its gradient) [4], whereas the contour energy function is usually given by an integral equation of high complexity.

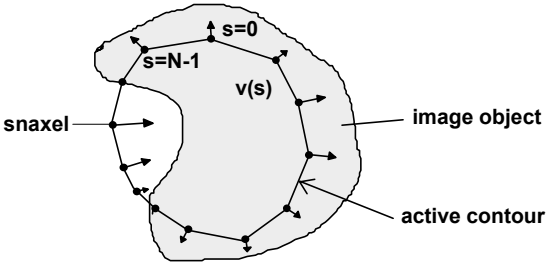

Fig. 1. Construction of an active contour model. The arrows represent directions of snaxels movements towards the borders of the analysed object.

In [10] an optimisation technique based on the Hopfield neural network has been proposed to deal with the problem of contour energy minimisation. Stable convergence of the contour energy to a minimum state was reported. However, because of a prohibitively large size of the network this method turns out to be computationally very costly, as hundreds of thousands of neurone nodes are required for edge detection tasks encountered in practice.

Another possible approach proposed in [9] is based on the idea that the initial potential energy of the contour E_{snake} is minimised using a technique in which a lower contour energy state is reached by converting its potential energy to a kinetic energy and then dissipating this kinetic energy through an energy dissipating function. Namely, a certain mass is associated with the moving contour which dissipates its kinetic energy due to the presence of some viscosity of an abstract environment in which the contour performs its motion. Accordingly, the following equation of contour motion is used to describe contour dynamics

$$m\frac{\partial^2 v(s,t)}{\partial t^2}+\gamma\frac{\partial v(s,t)}{\partial t}=\vec{F} \tag{2}$$

where m is the mass density of the contour, γ is the damping viscosity factor which accounts for contour energy dissipation and $\vec{F}$ represents intrinsic and external forces acting onto the contour which can be derived from contour energy function components as defined in (1). Using the equation of motion for description of contour dynamics allows for a fast determination of contour equilibrium state as it does not require seeking for the minimum of the total potential energy

function E_{snake} as given in (1). Computer implementation of the motion equation (2) requires that time, space domains and also other quantities characterising the contour must be discretised.

First, consider the discretisation of the parameter s used in a parametric description of an active contour given in (1). Instead of a continuous contour line one obtains a set of points called snaxels. It is convenient to define discrete domain of this parameter to be a set of integers in the range $\langle 0, S_m - 1 \rangle$, where S_m is the number of contour snaxels (for a better visualisation of the contour shape these points are usually connected by a straight line segments). Also, the image spatial domain, in which the contour is embedded and is defined by co-ordinates x and y, is discretised to reflect raster nature of a digital image. Hence, these co-ordinates assume values: $x = 0,1,..., X_m - 1$ and $y = 0,1,..., Y_m - 1$, where X_m and Y_m represent number of image pixels in the horizontal and vertical dimension correspondingly. In a similar fashion time domain is discretised to a numbered time instances $t = 0,1,..., T_m$ representing consecutive iteration steps of the active contour evolution.

A discrete version of the equation of motion, given for the continuous case in (2), will assume the following form, in which first and second order derivatives are substituted by respective differences:

$$m\frac{v(s,t) - 2v(s,t-1) + v(s,t-2)}{1} + \gamma\frac{v(s,t) - v(s,t-1)}{1} = \vec{F}(t-1) \tag{3}$$

where all the variables are as defined in (2) and assume discrete values.

This equation allows for an iterative computation of snaxels location for current time t on the basis of two previous contour locations at time instances *t-1*, *t-2* and on the value of force vector $\vec{F}$ at time *t-1*. Force vector $\vec{F}$ acting onto the contour is the sum of the forces minimising respective components of the contour energy E_{snake}. Thus,

$$\vec{F} = \vec{F}_{ext} + \vec{F}_{tens} + \vec{F}_{rig} + \vec{F}_{img} \tag{4}$$

where: $\vec{F}_{ext}$ is the force minimising snake energy component E_{ext} as introduced in (1) and (4), $\vec{F}_{tens}$ and $\vec{F}_{rig}$ are the forces resulting from contour tension and rigidity respectively and are associated with contour internal energy E_{int}, which they tend to minimise, $\vec{F}_{img}$ is the force vector derived from image brightness distribution designed to attract the contour to image salient features. Methods adopted for computing these forces are outlined below.

Force $\vec{F}_{ext}$ is computed as the derivative of the energy function E_{ext} in respect to the distance between contour snaxel and an arbitrarily chosen reference point encircled by the contour. If the energy function E_{ext} is chosen to be of the form (also see Fig. 2 for the plot of this energy function):

$$E_{ext}(r(s)) = -h_1 \ln(r(s)) + h_2 r^3(s) \tag{5}$$

the force associated with this energy is computed from the following relationship:

$$\vec{F} = \frac{\partial E_{ext}}{\partial r} = \left(3h_2 r^2 - \frac{h_1}{r} \right) \left[\frac{x - x_0}{r} \; \frac{y - y_0}{r} \right]^T \tag{6}$$

where *r(s)* is the distance between points belonging to the contour and an arbitrarily chosen reference point encircled by the contour. This distance is calculated from:

$$r = \sqrt{(x - x_0)^2 + (y - y_0)^2} \tag{7}$$

where: *(x, y)* and *(x_0, y_0)* are coordinates of the contour point and a predetermined reference point respectively. Note that the direction of the force $\vec{F}$ depends on the relative location (x,y) of the considered snaxel with respect to the contour reference point. For the E_{ext} energy function, as proposed in Fig. 2, this force is an expanding force for $r < 0.9$ and a contracting force for $r > 0.9$.

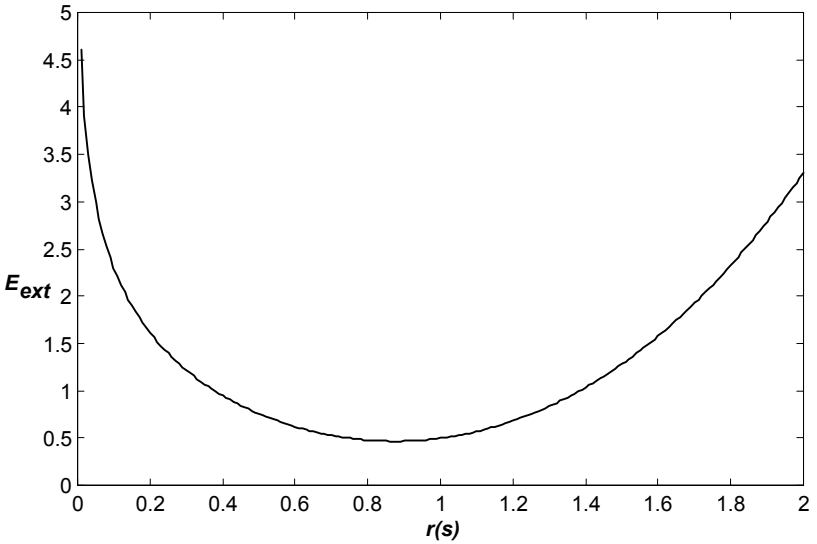

Fig. 2. Plot of energy function E_{ext} given by Eq. (4) for coefficients $h_1 = 1$ and $h_2 = 0.5$ versus the normalised distance between the contour point and the contour reference point.

Similarly, it is assumed that direction of the $\vec{F}_{img}$ force activity is limited to the line connecting the considered snaxel with the contour reference point. Assuming that image brightness distributions of the object for which the edge is searched for and the brightness distribution of the background are approximately known, some threshold value J_c between the two brightnesses can be chosen to compute the force $\vec{F}_{img}$. The following relationship was used in the reported work:

$$\vec{F}_{img} = J_w\left[J(x,y) - J_c\right]\left[\frac{x-x_0}{r}\ \frac{y-y_0}{r}\right]^T \tag{8}$$

where J_w is the coefficient (either positive or negative) defining the magnitude and direction of the $\vec{F}_{img}$ force, and *J(x,y)* is the image brightness which coincides with the considered snaxel location. It is worth adding that this force is the only image dependent information used in the computations of active contour shape.

The forces associated with contour internal energy will be derived on the basis of equation (9).

$$E_{\text{int}}(v(s)) = 2w_1\left|\frac{\partial v(s)}{\partial s}\right|^2 + 2w_2\left|\frac{\partial^2 v(s)}{\partial s^2}\right|^2 = 2w_1E_{tens} + 2w_2E_{rig} \tag{9}$$

where weight w_1 regulates contour tension energy E_{tens} (i.e. its resistance to stretching) and weight w_2 regulates contour rigidity energy E_{rig} (i.e. its resistance to bending).

First, consider contour internal energy component E_{tens} responsible for contour tension. For a chosen snaxel *s*, influences of adjacent snaxels *s-1* and *s+1* need to be accounted for (as suggested by the differential equation (9)). For the discrete case one gets:

$$E_{tens}(v(s)) = w_1[v(s) - v(s-1)]^2 + w_1[v(s+1) - v(s)]^2 \tag{10}$$

where w_1 is the scaling factor as defined in (9). This energy reaches minimum, i.e. $\partial E_{tens}/\partial s = 0$, for $v(s) = \dfrac{[v(s+1) + v(s-1)]}{2}$. Thus, it is convenient to use the following expression for contour tension force:

$$\vec{F}_{tens} = W_1\left[\frac{v(s+1) + v(s-1)}{2} - v(s)\right] \tag{11}$$

where W_1 is a scaling factor proportional to w_1. Very similar reasoning carried out for the contour internal energy component E_{rig} yields the final relationship for the rigidity force:

$$\vec{F}_{rig} = W_2\left[\frac{v(s+2) + v(s-2) - 4[v(s+1) + v(s-1)]}{6} - v(s)\right] \tag{12}$$

where W_2 is a scaling factor proportional to w_2. Now, once all the expressions for computing considered forces are given, it remains to sum them up and substitute for the right hand side of contour motion equation (3). After transformation of that equation to get the final formula for contour snaxels co-ordinates for the current time *t* one obtains:

$$v(s,t) = \frac{2mv(s,t-1) - mv(s,t-2) + \gamma v(s,t-1) + [\vec{F}_{ext} + \vec{F}_{tens} + \vec{F}_{rig} + \vec{F}_{img}]}{m + \gamma} \tag{13}$$

This relationship allows for iterative computations of successive contour positions by using their previous positions from iterations *t-2, t-1* and forces computed at *t-1*. Although, after appropriate expressions are substituted for force vectors, this equation seems complex, in fact however, it

requires simple calculations only. Hence, in case of computer implementations this method is relatively fast if one considers that on average less that 100 computing iterations of (13) suffice for the active contour model to reach its equilibrium state.

3. Modifications of the active contour model

Practical applications of the active contour model to a number of artificial test images and real world images have revealed that proper choice of contour parameters (i.e. coefficients of equations (2), (5) and (9)) is critical for successful contour detection. Unless these parameters are correctly tuned the following problems may occur:

- contour oscillations in case of incorrect choice of contour tension and coefficients used for construction of E_{image} energy (see Fig. 3),

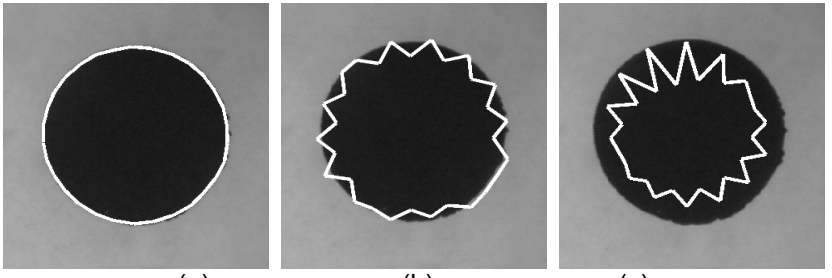

Fig. 3. Contour oscillation effects: correct matching to image object (a), too large a contrast of the image (b), too large a value of contour tension parameter (c).

- contour shrinkage or unbounded expansion in case of incorrect choice of coefficients defining external constraints put onto contour energy E_{ext},
- the effect of pulling the contour towards one side of the image object boundary; this frequently occurs for images characterised by areas of uniform brightness for which values of energy E_{image} hardly vary and contour points can freely migrate within the object area (see Fig. 4),
- problems in fitting snake shape to objects characterised by complex shapes, in such cases extra forces have to be defined to aid snake shape forming process [6], this however adds an extra degree of freedom to snaxels motion and imposes an additional computing burden to the edge finding procedure.

In the sections to follow, two novel modifications of the original active contour model are introduced. Both of them deal with the changes made to the degrees of freedom allowed to snaxels motions.

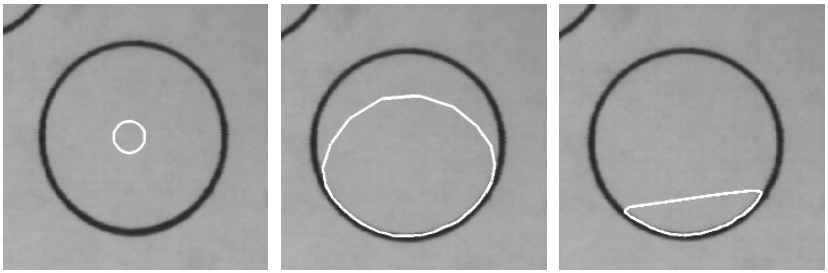

(a) (b) (c)

Fig. 4. The pulling effect of the contour towards one side of the object: after contour initialisation (a), after 40 iteration steps (b) , after 100 iteration steps (c).

3.1. Central contour model

This modification, introduced to the original active contour model, is aimed at simplifying the computational procedure so that the contour dynamics could be more easily controlled. This method which was termed *central contour model* relies on the idea that motion of the contour points takes place along a predetermined number of fixed radial lines which originate from an arbitrary chosen contour central point (see Fig. 5a). It is proposed that these radial lines are equally spaced in terms of angles formed between them to cover the full 2π angle. Hence, if the number of radial lines is S_m, the number of contour points (termed in such a discrete case *snaxels*) is also S_m and the angular distance between adjacent radii is $2\pi/S_m$. Following these assumptions, spatial co-ordinates of each contour snaxel (required in the equation of motion (2)) can be computed from the following simple relationship:

$$\begin{cases} x(s) = x_0 + r(s)\sin\dfrac{2\pi s}{S_m} \\ y(s) = y_0 + r(s)\cos\dfrac{2\pi s}{S_m} \end{cases} \tag{14}$$

where x_0, y_0 are the co-ordinates of the arbitrarily chosen contour central point, S_m is the number of contour snaxels, s is the snaxel number, i.e. $s=0, 1,..., S_m-1$, and $r(s)$ is the radial distance of snaxel s from the central point.

The central point indicates the location within the object area at which an active contour of some small predefined size is initialised. Then contour dynamics, which is defined by equation of motion (2), makes the contour grow in size until it reaches its equilibrium state. The proposed constraint of snaxels motion along a limited number of radial lines makes that this version of the original active contour model has less degrees of freedom and consequently its implementation is faster. Moreover, it has made it possible to eliminate contour pulling effect as pointed out earlier and illustrated in Fig. 4. This is because, as opposed to the original algorithm, in the central contour model the contour points can not migrate in all possible directions, e.g. they can not cross the location of the central point or move around it. Snaxels can only shift their position

along the radial lines and when they attempt to approach the central point they are repelled by large values of energy E_{ext}.

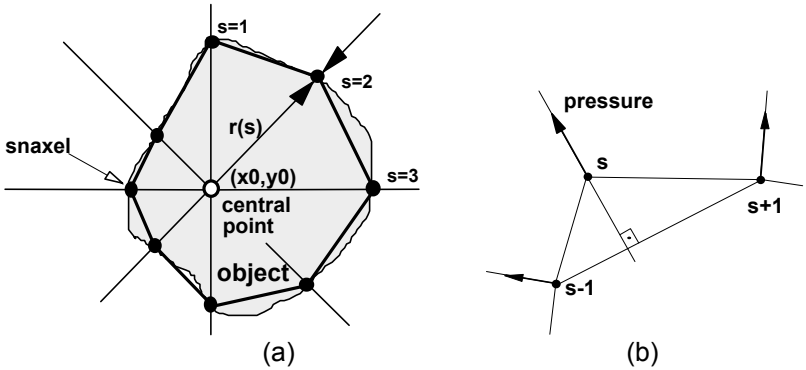

Fig. 5. Illustration of active contour model modifications: central contour model (a), pressure model (b).

Finally, it should be stressed that application of the central contour model is not limited to convex shapes only. Edge extraction of concave shapes can also be realised using this method provided that the radial lines snaxels are shifted along, cross the object border no more than once. Additionally, for more complex shapes for which this condition cannot be met, more than one central point can be used. Each central point should be connected with a subset of the snaxels so extending model capability in extracting edges of complex shapes like spiral, asterisk etc.

3.2. Pressure contour model

Another approach aimed at extending active contour capabilities to account for situations, in which edges of complex shapes need to be extracted is proposed here. This method is termed *pressure contour model*.

Assume the forces influencing contour snaxels, which correspond to the energy E_{ext} are kept perpendicular to the contour line. Hence, the energy E_{ext} is minimised by moving contour points in the direction perpendicular to its local line fragments. This resembles the process of balloon expansion in response to the gas pressure force acting onto it. In order to mimic such a process, the force vector should be directed to the exterior of an object under analysis. In the proposed method it is assumed that the value of this pressure force (i.e. the length of the corresponding vector) which is applied to each of the snaxels is constant during entire iteration process, i.e. it does not depend on the contour size and shape. Fig. 5b explains the idea lying behind this simple, yet effective version of an active contour model for a discrete case.

The introduced modification allows to "pump" contour snaxels into object fragments outlined by complicated edge curvatures (e.g. spirals) without the need of defining multiple snake reference points. Numerical implementations of the pressure contour model have revealed however, that directions of the pressure forces have to computed with high accuracy. Otherwise a

"looping" effect as shown in Fig. 10 can take place. In order to minimise the risk of this negative phenomenon it is advised keep adjacent snaxels not too close to each other so that the computation of the perpendicular direction to the contour is based on a larger contour fragment.

4. Results

An active contour model and its modified versions were tested on images of different classes. These images were artificial test images and real world images. Edge information in images of the specially selected classes is either noisy or changes its characteristics across the image and hence edges are difficult to track by standard and non adaptive image processing techniques [7].

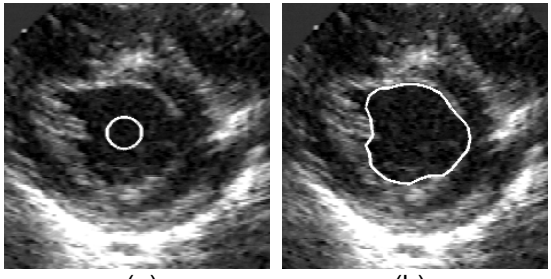

(a) (b)

Fig. 6. Detection of heart wall boundaries during systole: contour initialisation (a), final contour position (b).

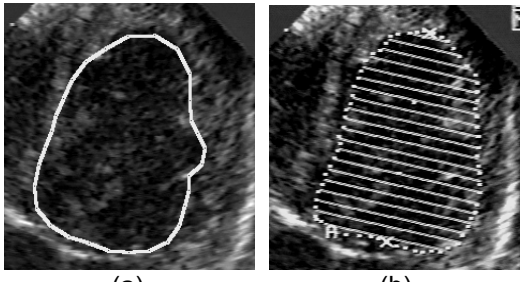

(a) (b)

Fig. 7. Echocardiographic images in which the cardiac boundaries (for heart diastole) were extracted: using an active contour model (a) and manually by the clinician (b).

The first type of the processed images were echocardiographic scans. As illustrated in Fig. 6 these images are characterised by a low spatial resolution and contain high level speckle noise. Also, some anatomical features of the scanned heart are not equally well represented in the image, particularly in the areas where the incident ultrasound beams are parallel to the cardiac muscle walls. Thus, the diagnosis objective aimed at detection of edges corresponding to heart muscle

walls is a non-trivial image analysis task. Location of heart muscle boundaries serves as a basis for measurements of heart chamber volume, estimation of blood volume pumped etc. [11].

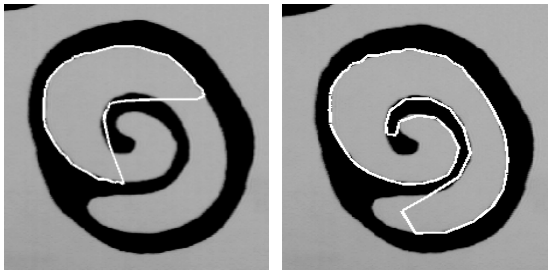

(a) (b)

Fig. 8. Edge extraction of complex object shape: with the use of the standard active contour model (a), after application of the pressure contour model (b).

Fig. 6 illustrates the application of the central contour method for heart wall boundaries extraction during cardiac systole. Left panel depicts the initial shape of the contour and the right panel the final steady state reached by the contour. In Fig. 7 the performance of the central contour model in detecting image edges in echocardigraphic scans (left panel) is compared to the result (right panel) obtained when the same task is performed manually by a skilled cardiologist. Although, some details of the obtained contours do not match precisely the general shape of the heart chamber section (shaded area in the right panel) compares favourably. Note however, that the contour indicated manually, as it is currently done in clinical setting, is not a perfect approximation of the real boundary of the analysed object.

For the contours presented in Figs. 6 and 7 an active contour consisting of 30 snaxels is used. Contour position viewed in the left panel of Fig. 6 is obtained after 60 iterations (about 1 s of PC/486 50 MHz computing time), after which the contour has reached its equilibrium state.

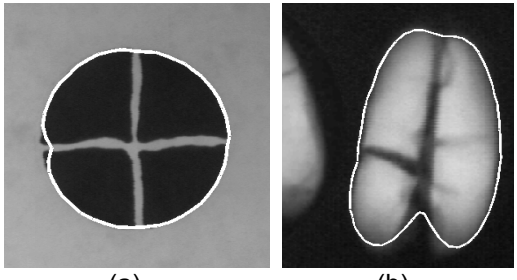

(a) (b)

Fig. 9. Edge extraction of image objects characterised by a non-uniform brightness distribution: for an object composed of four disjoint quadrants (a), for the X-ray image of a cracked grain (b).

Other types of images on which the active contour model was tested, were images characterised by non convex shapes and with non-uniform boundaries. Fig. 8 illustrates a spiral shaped object and the results obtained when a standard (left panel) and modified pressure contour model (right panel) were used. Whereas the standard model failed completely in detecting such a complex object boundary the pressure model yielded acceptable results.

Two other examples of the modified central contour model performance are illustrated in Fig. 9. The left panel contains a specially prepared test object composed of four disjoint quadrants. The central contour method managed to detect external boundary of such an object. This result, represented by the superimposed solid white line of the contour was possible to obtain due to existence of contracting forces between contour snaxels.

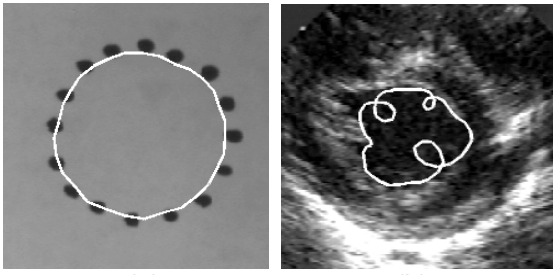

Fig. 10. Active contour model capabilities to interpolate non-continuous image edge (a) and an undesired contour behaviour for incorrectly set pressure contour model parameters (b).

Capabilities of the active contour model to detect non uniform boundaries have been also found useful in the analysis of X-ray images of grains. The right panel of Fig. 9 depicts the grain which suffered from clearly visible cracks due to the drying process. The objective is to evaluate the quality of a grain in terms of the number and severity of their cracks. The first step in such an analysis is detection of the grain boundary in the image. Note that the method of active contour model performed correct grain boundary extraction in spite of a non-uniform image brightness distribution within the area of the cracked grain. Currently, a final version of a specialised computer program for analysis of X-ray images of grains is being developed at the Institute of Electronics, Technical University of Łódź in cooperation with Institute of Agrophysics in Lublin, the Polish Academy of Sciences. The method of the active contour model for detection of grain boundaries in X-ray images proved very useful; it is fast, precise and reliable.

Finally, it is important to highlight one of the most important features of the active contour model, that is, the capability to interpolate non-continuous image edges as demonstrated in Fig. 10a. Such an excellent result, which has been obtained with the use of the central contour model, is provided by the existence of contour internal forces (tension and rigidity forces).

Results demonstrated in Figs. 6÷10a were obtained with the same, default set of model parameters which are given in the middle column of the table included in the Appendix (except for image related coefficients as explained in section 2). These parameters were chosen to give

good results on different types of images. Presented results can still be improved if parameter values are specially tuned for each single type of analysed image objects.

5. Summary and conclusions

The method of an active contour model suited specifically for extraction of fuzzy and broken image edges/boundaries has been presented along with the two novel modifications of the original model. The main strength of such energy minimising curve methods for image edge extraction is that they produce continuous contours not guaranteed by other standard image processing techniques. (see Figs. 6 and 7). These methods can also be applied for extracting boundaries of non-uniform characteristics and used for interpolation of non-continuous edges (see Figs. 6, 7 and 9, 10a). Additionally, contour information is obtained from the method in the form of a set of ordered snaxels co-ordinates, which is convenient for further processing and analysis.

Two modifications to the original active contour model have been proposed. The first, termed *central contour model*, is aimed at simplifying the algorithm so that computations required for contour simulation are faster. It is based on the idea that motion of contour points is restricted to the direction along the radial lines which connect snaxels with the contour central point. Because snaxels have less degrees of freedom this method is faster in computer implementation and its parameters are easy to control. Introduction of the second modification, termed *pressure contour model*, has simplified the procedure for extraction of object boundaries characterised by complex shapes, e.g. spirals, as demonstrated in Fig. 8.

It has to be noted that the key point to successful application of active contour models is correct choice of the contour model type and its parameters (see e.g. Fig. 10b illustrating looping of the contour line in the contour pressure model for which the direction of pressure forces were incorrectly calculated) . Tuning of contour parameters is an image specific process and has to be performed for each of the analysed image types. However, once contour model is optimised, good quality results of contour extraction may be expected for the image class under consideration.

Because active contour methods are fast and reliable and because extraction of image edges is a fundamental problem in image analysis, the presented methods can prove useful in most computer vision applications, like medical diagnosis, robotics, industrial quality control, food industry, etc.

Appendix: Active contour model parameters

The table below contains listing of the parameters used in the computer simulations of the active contour model. For convenience of the program user, most of the parameters were scaled to the range <0, 100>. Scaling factors used for obtaining this range from the true values of the parameters (which in fact are used in calculations) are indicated in the right hand column of the table (if no scaling factor is given it is assumed to be unity). Majority of the results presented in the paper were obtained for parameter values contained in the column under the heading ”default”.

Tab. A. A set of model parameters.

Parameter name	Value			Scaling
	min.	default	max.	
Number of snaxels	3	30	127	S_m
Distance	1	16	200	r
Tension	-100	20	100	$32\times u_1$
Rigidity	-100	8	100	$128\times u_2$
Viscosity	0	36	100	γ
Mass	1	3	100	$16\times m$
Contrast coefficient	-400	100	400	$32\times J_w$
Coefficient h_1	-100	22	100	$128\times h_1$
Coefficient h_2	0	2	100	$512\times h_2$
Threshold level	1	~	254	J_c

Acknowledgements

Authors wish to thank Dr E. Makowiecka from the Polish Mother's Health Centre for providing video recordings of the echocardiographic scans and Dr J. Niewczas from the Institute of Agrophysics of the Polish Academy of Sciences in Lublin for supplying X-ray images of grains.

References

1975

[1] S. Davis, A survey of edge detection techniques. CGIP, 4:248-270, 1975

1980

[2] Marr and E. Hildreth. Theory of edge detection. Proc. Of the Royal Society, B-207: 187-217,1980.

1986

[3] J. Canny. A computational approach to edge detection. IEEE Trans. PAMI, 8(6): 697-698, 1986.

1987

[4] G. Dahlquist, A. Björck, *Numerical Methods*, WNT, Warszawa, 1987 (Polish edition).

1988

[5] J. Illingworth and J. Kittler. A survey of the Hough transform. CVGIP, 44:87-116, 1988.

[6] M. Kass, A. Witkin, D. Terauzopoulos, *Snakes: Active Contour Models*, International Journal of Computer Vision, vol. 1, no. 4, pp. 321-331, 1988.

1989

[7] A. K. Jain, *Fundamentals of Digital Image Processing*, Prentice-Hall, 1989.

1992

[8] A. Kuriański. Time-varying corners in practical application - discussion. MG&V,1(3):527-536, 1992.

[9] F. Leymarie, M. D. Levine, *"Simulating the Grassfire Transform using an Active Contour Model"*, IEEE Transactions on Pattern Analysis and Machine Intelligence, vol. 14, no. 1, January 1992, pp. 56-75.

1993

[10] C. T. Tsai, Y. N. Sun, P.C. Chung, *Minimising the Energy of Active Contour Model using Hopfield Network*, IEE Proceedings-E, vol. 140, No. 6, November 1993, pp. 297-303.

1994

[11] H. Feigenbaum, *Echocardiography*, Lea & Febiger, 1994.

[12] S. R. Gunn, M. S. Nixon, *A Dual Contour incorporating Parametric Shape Description*, Proceedings of EUSIPCO-94, Seventh European Signal Processing Conference, Edinburgh, U. K., September 1994, vol. 1, pp. 435-438.

[13] K.M. Lam, H. Yan, *Fast Greedy Algorithm for Active Contours*, Electronic Letters, January 1994, vol. 30, no. 1 , pp. 21-23.

1995

[14] L. Chmielewski. A note on merging line segments with the search space reduced by a condition based on an ordering, MG&V, 4(1-2):29-38, 1995.

[15] P. Strumiłło, P. Szczypiński, *Automatic Extraction of Fuzzy and Broken Image Edges using Active Contour Model*, Proceedings of the XXVIII-th National Conference, Circuit Theory and Electronic Networks, Polana Zgorzelisko, Poland, October 1995, pp. 485-490.

[16] P. Szczypiński, *Image Segmentation using an Active Contour Model*, M.Sc. Thesis, Technical University of Łódź, 1995 (in Polish).